Short-time Lyapunov exponent analysis

By J. A. Vastano

A new technique for analyzing complicated fluid flows in numerical simulations has been successfully tested. The analysis uses short-time Lyapunov exponent contributions and the associated Lyapunov perturbation fields. A direct simulation of Taylor-Couette flow just past the onset of chaos demonstrated that this new technique marks important times during the system evolution and identifies the important flow features at those times. This new technique will now be applied to a "minimal" turbulent channel.

1. Introduction

Numerical simulations of turbulence are increasing in number and quality each year. These simulations provide a wealth of information about the structure of turbulent flows. The analysis of these flows must start, therefore, by discovering when and where to look at the system in order to see the important events in the flow evolution. Short-time Lyapunov exponent analysis is a new technique that shows promise for finding these events. Research at the Center for Turbulence Research over the past year has shown that this technique can successfully locate the times during a flow evolution when important chaos-producing mechanisms are operating. At these times, the structure of the perturbation fields associated with the Lyapunov exponent computation give a picture of those flow features in which the exponential growth of perturbations is occurring. This report will define the Lyapunov exponent spectrum, describe the short-time contributions and fields used in the analysis, and discuss the numerical tests that have been performed.

2. Lyapunov exponent analysis

The asymptotic motion of a bounded, dissipative system is on some attracting set in its phase space (Eckmann and Ruelle 1985). Attractors range from simple fixed points to chaotic strange attractors. The Lyapunov exponent spectrum provides a fundamental description of the geometric and dynamical properties of an attractor. Lyapunov exponents measure the long-term average exponential growth rate of perturbations to the system trajectory in phase space. More precisely, if the time evolution of the system x is given by

$$\dot{x} = F(x),$$

then a perturbation δx evolves according to

$$\dot{\delta x} = J(x)\delta x;$$

where $J(x)$ is the linearized form of $F(x)$, $J(x) = dF/dx$. For a given initial condition $x(0)$ on the attractor and an initial perturbation $\delta x(0)$,

$$\delta x(t) = M(t, x(0))\delta x(0),$$

where

$$M = \int_0^t J(x(s))ds$$

The long-time evolution of perturbations will be governed by the eigenvalues of M^*M. The eigenmodes specify perturbation fields $\delta x_i(0)$ that will grow at the rates given by the eigenvalues. We define the Lyapunov exponents λ_i by

$$\lambda_i = \lim_{t\to\infty} \frac{1}{t} \log(|\delta x_i(t)|/|\delta x_i(0)|).$$

The exponents are ordered so that λ_1 is largest. There are an infinite number of Lyapunov exponents for a spatially-extended system. Each exponent corresponds, roughly, to a separate direction in phase space. The Kaplan-Yorke conjecture (Frederickson et al. 1983) gives a simple formula that relates the Lyapunov exponents of an attractor to its dimension. Initial perturbations in almost any direction will grow at the rate λ_1, but there exist subspaces of the initial tangent space for which perturbations grow at the rates given by the other Lyapunov exponents as well. In computing the exponents, one follows N perturbations to estimate N Lyapunov exponents. A standard technique exists for evolving the perturbations for long times and obtaining estimates of all N exponents (Benettin et al. 1980) The basic procedure is the Gram-Schmidt reorthogonalization, which removes from the i-th perturbation field those components corresponding to growth at rates λ_1 through λ_{i-1}.

The greatest difficulty in computing Lyapunov exponent spectra for model systems is that the convergence of the running estimates to the long-time average exponents is slow (like $1/t$) and cannot be accelerated. On the other hand, it has been argued (Goldhirsch et al. 1987, Greene and Kim 1987) that the evolving perturbation fields $\delta x_i(t)$ decay exponentially fast to the eigenmodes of $M(t, 0)$ and, furthermore, that these functions are themselves a smooth field over the attractor. In other words, the Lyapunov perturbation fields are local properties on the attractor. If this is the case, then the short-time contributions to the long-time average exponent,

$$\Delta\lambda_i(t) = \frac{1}{\Delta t} \log(|\delta x_i(t + \Delta t)|/|\delta x_i(t)|)$$

are also local properties on the attractor.

The growth of perturbations to the system at any time can be measured by projecting the perturbation onto the local Lyapunov perturbation fields and

checking the short-time expansion rates. Clearly, when these short-time rates are much smaller or larger than average, perturbation will either be damped or expand at large rates. In addition, if the perturbation fields themselves have structure, they indicate where in physical space the mechanisms driving the instability are located, and the form of the instability.

3. A test case

To test the utility of the short-time exponent analysis, numerical simulations were performed on Taylor-Couette flow just past the onset of chaos in that system. This system was chosen because there is experimental evidence that the flow is low-dimensionally chaotic at computationally accessible Reynolds numbers. A code for computing the base flow already existed (Moser et al. 1985) and could be easily extended to the computation of N Lyapunov exponents. Although there had been a great deal of previous experimental, theoretical, and numerical work on this system, the transition to chaos was not understood. In particular, no physical mechanism or instability underlying the transition from quasiperiodic to chaotic flow had been determined.

The particular Taylor-Couette flow studied was chosen to match the most complete experiment to date on the transition to chaos in this system (Brandstater et al. 1985, Brandstater and Swinney 1987). For this case, the outer cylinder is fixed and the inner rotates at a constant frequency. At Reynolds numbers R near zero, the flow state is Couette flow, axially and azimuthally homogeneous. At a critical Reynolds number R_c, a bifurcation to another steady flow occurs. This is Taylor vortex flow, consisting of an axial stack of ring vortices, still azimuthally homogeneous. Neighboring vortices rotate in the opposite sense, so that vortices are separated by alternating inflow and outflow boundaries. The axial wavelength is defined by a pair of Taylor vortices. In the experiment of Brandstater and Swinney, the average axial wavelength was 2.5 times the gap between cylinders. The numerical simulation assumes axial periodicity; the axial period is set to 2.5 gaps.

At higher Reynolds numbers, first one and then a second azimuthal travelling wave appear on the vortices. Each travelling wave introduces an independent frequency of motion to the flow. The waves have integer azimuthal wavenumber: in the experiment of Brandstater and Swinney, both travelling waves had wavenumber four. This is convenient for the simulations, since the state is fourfold symmetric in the azimuthal direction and it is only necessary to simulate a quarter of the azimuthal extent. In the experiment, the onset of quasiperiodic (two-frequency) flow occurred at $R/R_c = 10.0$, and a chaotic flow was observed at $R/R_c = 11.7$. The dimension of chaotic attractors can be determined from time series data. Experimental time series yielded dimension estimates between two and three for Reynolds numbers as high as $R/R_c = 15$.

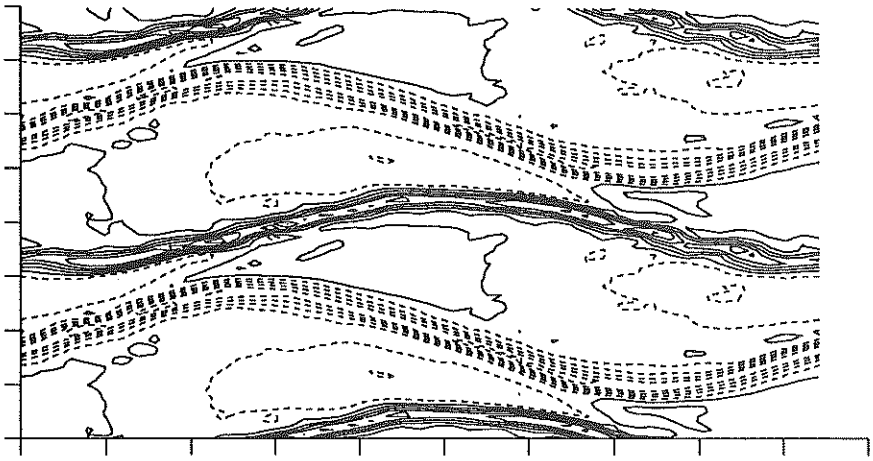

FIGURE 1. Contours of azimuthal velocity at a midplane in r for $R/R_c = 12.0$. The horizontal axis is the azimuthal direction and the vertical axis is the axial direction. One-quarter of the cylinder is shown azimuthally, and two axial wavelengths (twice the computational grid) are shown axially.

4. Results

To convert the code of Moser et al. to estimate N, Lyapunov exponents required following $N + 1$ times as many fields. The linear part of the time evolution operator is identical for the base flow and the perturbations. The nonlinear term of the evolution operator for the base flow is $u \times \omega$. For the perturbations, this term becomes $\delta u \times \omega + u \times \delta\omega$. The only other addition to the code was the Gram-Schmidt reorthogonalization procedure, which is done every few time steps, primarily to give smooth short-time contribution curves. Since computing N Lyapunov exponents requires $(N+1)$ times as many grid points as does the base simulation, it was essential to use the lowest resolution possible. The resolution used in the simulations was 16 Chebyshev modes radially by 32 Fourier modes in the axial and azimuthal directions. This resolution was sufficient to capture the flow in the quasiperiodic regime immediately prior to the onset of chaos with good accuracy. The travelling wave frequencies were predicted to within 2% of the values seen in experiment at $R/R_c = 11$. Increasing the number of radial modes to 32 dropped the discrepancy to less than a percent, but did not otherwise alter the flow.

A sample flow visualization, at $R/R_c = 12$, is shown in Figure 1. This is a picture at an instant of time of a chaotic flow. The quantity shown is the azimuthal velocity component of the flow at a radial midplane. The more focused, higher velocity jet is the radial outflow boundary jet, while the more diffuse

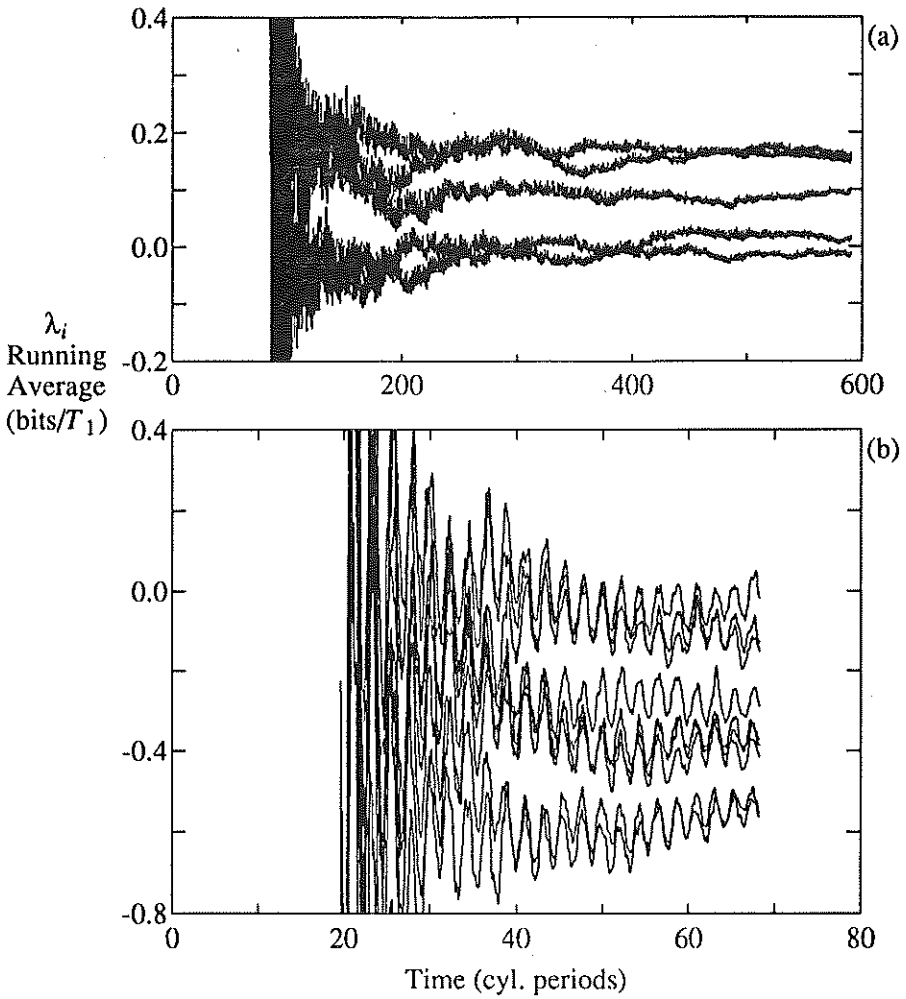

FIGURE 2. Convergence of the Lyapunov exponents at $R/R_c = 11.32$ for (a) the first five exponents, (b) exponents six through fourteen.

jet is the radial inflow boundary jet. The jets are labelled by their radial components, but the dominant velocity component in both jets is azimuthal, not radial. Chaos appeared in the simulations at about $R/R_c = 11.1$, earlier than had been observed in experiments. A power spectral analysis of a numerically computed time series showed that the travelling wave peaks in the spectrum corresponding to the travelling wave frequencies were about 8 decades above the broadband noise component at $R/R_c = 11.3$. The experiments had only six decades of signal-to-noise separation; thus, it is probable that the chaos was already present in the experiment at this Reynolds number, but was masked by the instrumental noise.

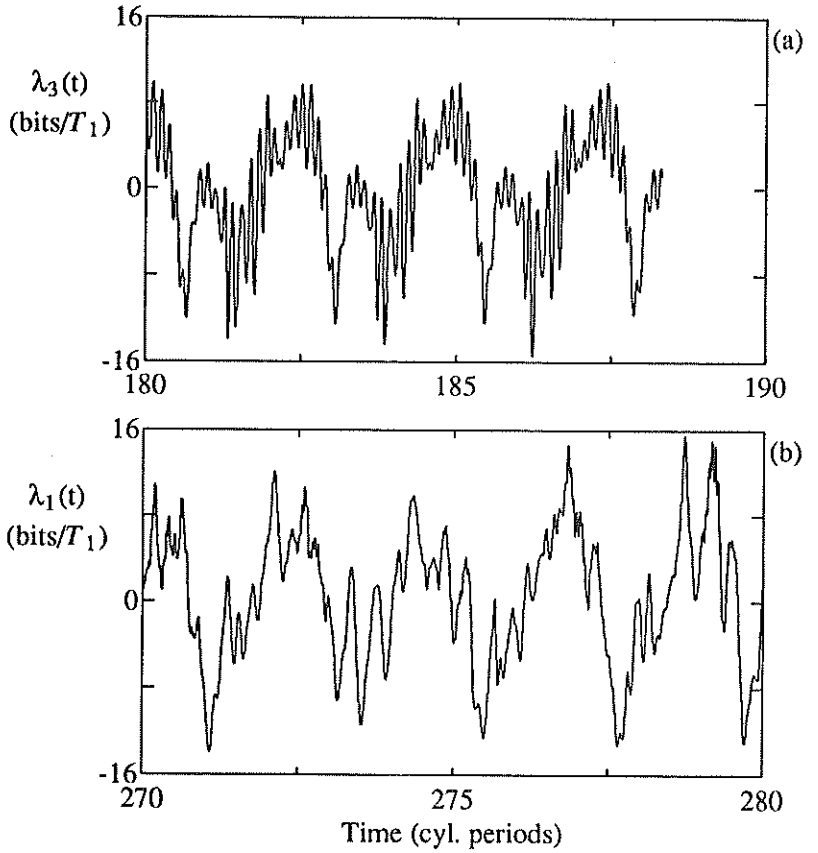

FIGURE 3. Short-time contributions to the first nonzero Lyapunov exponent for (a) $R/R_c = 9.71$ (quasiperiodic), and (b) $R/R_c = 11.32$ (chaotic).

The convergence of the Lyapunov exponents in the simulation is shown in Figure 2. The first five exponents were computed for almost 600 cylinder revolutions, but clearly from the figure they are just converging. The next nine exponents were followed for a much shorter time, and there is still a large uncertainty in their estimates. The trend in the exponents is clear, however, and the Kaplan-Yorke formula gives an attractor dimension of about nine. This is higher than the values between 2 and 3 determined from experimental data. It would appear that low amplitude structure unresolved in the experiments adds significantly to the dimension of the chaos.

Computation of well-converged Lyapunov exponent spectra is expensive: the runs described above used more than 500 hours of CPU time on a Cray-YMP computer. This is in contrast to the short-time Lyapunov exponent contributions, shown in Figure 3 for a quasiperiodic and a chaotic case. The perturbation fields, started from random initial conditions, evolved very rapidly towards

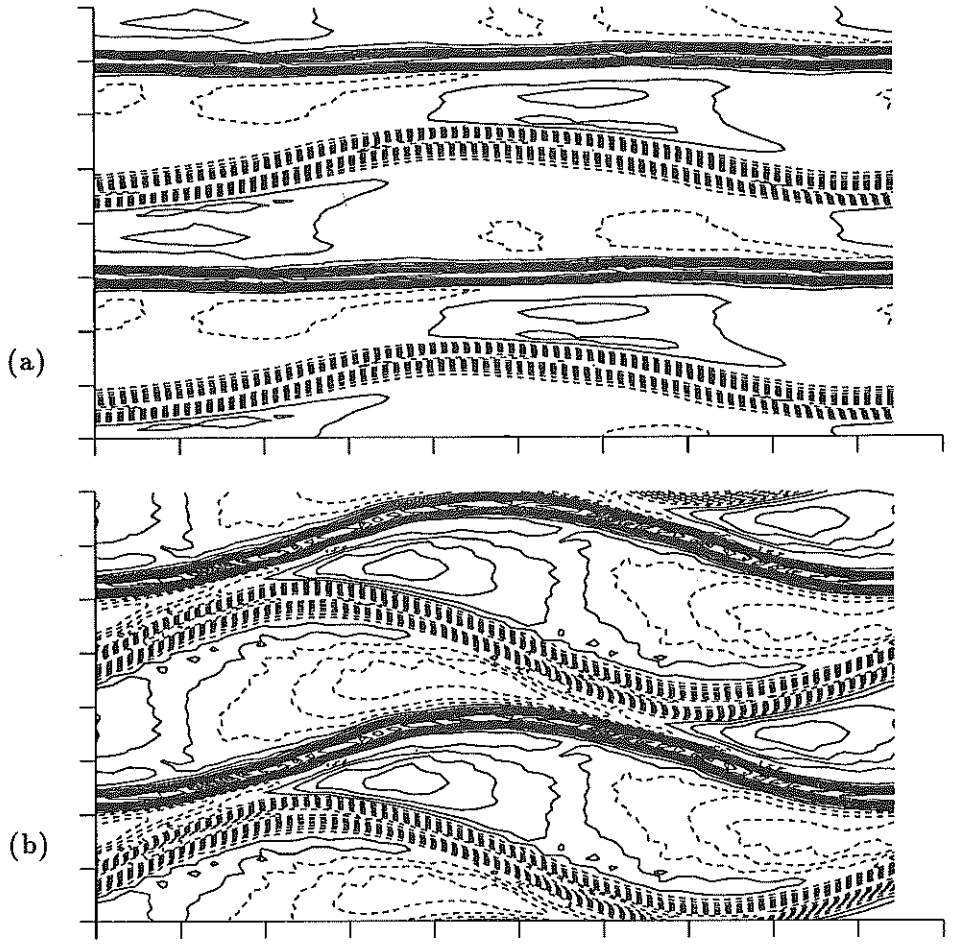

FIGURE 4. The chaotic flow at $R/R_c = 11.32$. Shown are the azimuthal velocity contours at a midplane in r for (a) a minimum in the short-time contributions to λ_1, and (b) a maximum.

asymptotic forms that are displayed at selected times for the chaotic case in Figure 5. The short-time contributions settled down somewhat more slowly than the gross form of the perturbation fields, but were qualitatively similar to the time traces shown in Figure 3 within 40 cylinder revolutions.

The first thing to notice about the short-time contributions is the enormous variation of the contributions compared to the long-time average exponents. For the quasiperiodic case, the contributions are to the first negative exponent, which has a value of -0.4 bits/T_1, where T_1 is the period of the primary travelling wave. For the chaotic case, the contributions shown are for the first exponent, which has a value of 0.35 bits/T_1. The short-time contributions can be forty times or

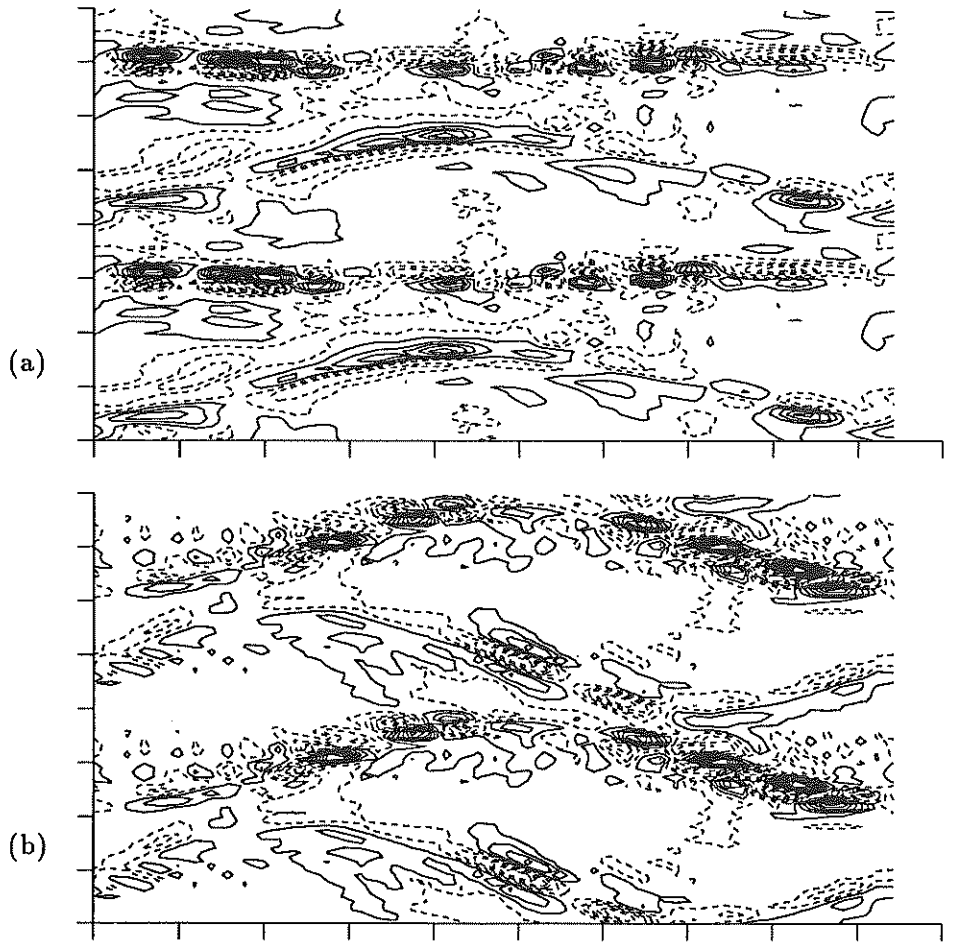

FIGURE 5. The perturbation field corresponding to λ_1 for the flow of Fig. 4. Shown are the azimuthal velocity contours at a midplane in r for (a) a minimum in the short-time contributions to λ_1, and (b) a maximum.

more the size of the long-time average, and of either sign. There are fairly rapid, small oscillations in the contributions that are not yet understood; they may be related to the evolution of structures in the perturbation fields. The large scale oscillations on a time scale of two cylinder periods are the important features for understanding the flow. At minima, perturbations to the flow are crushed, while at maxima they can expand at an enormous rate (for a short time). Figure 4 shows the chaotic flow at times corresponding to a minimum and the succeeding maximum of the short-time contributions to λ_1. The large-scale change in the wave-forms is the quasiperiodic part of the flow. The separation of the outflow and inflow jets at closest approach is much smaller at the maximum time than at

the minimum time. This seems to be what triggers the instability of the flow that causes the chaos. The jet profiles have been followed as they evolve, and there does not appear to be any change in the jets other than their separation. The nature of the instability that is triggered can be seen in Figure 5, which displays the perturbation field at the same times. All of the energy in the perturbation is concentrated on the outflow boundary jet at both times, and it has the same general form: the outflow jet is rolling up. Examination of the perturbation field at other radial locations shows no important radial effects, so while the jet is not two-dimensional, the instability is very much a Kelvin-Helmholtz type phenomenon.

The instability scenario gleaned from the short-time analysis is this: as the quasiperiodic evolution of the flow proceeds, the outflow jet is destabilized by the close approach of the inflow boundary jet. For some part of the overall evolution, a perturbation of the outflow jet in the form of a roll-up of the jet can grow. This produces the chaos in the system. Examination of Figure 1 shows that at higher Reynolds numbers, the roll-up becomes more apparent in the base flow itself. The same type of perturbation field is also observed for the quasiperiodic case, indicating that prior to the instability, the same mechanism is present as a damped mode.

5. Future plans

The test case has shown that short-time Lyapunov exponent analysis can be a useful tool for examining chaotic flows. The next step will be to apply this tool to a fully turbulent flow. The plane channel case studied by Keefe (1987) has an extremely high dimension, requiring the evolution of many hundreds of perturbation fields. This will not be possible in an economical way. A better alternative is the "minimal" channel studied by Jiménez (1989): not only will the dimension and thus the number of requisite perturbations be lower, but the number of structures in the flow will be reduced, simplifying the task of identifying which of them are important to the turbulence evolution

REFERENCES

BENETTIN, G., GALGANI, L., GIORGILLI, A., & STRELCYN, J.-M. 1980 Lyapunov Characteristic Exponents for Smooth Dynamical Systems . *Meccanica.* **15**, 9.

BRANDSTATER, A., SWIFT, J., SWINNEY, H. L., WOLF, A., FARMER, J. D., JEN, E., & CRUTCHFIELD, J. P. 1983 Low-Dimensional Chaos in a Hydrodynamic System. *Phys. Rev. Lett.* **51**, 1442.

BRANDSTATER, A. & SWINNEY, H. L. 1987 Estimating the dimension of strange attractors. *Phys. Rev. A.* **35**, 2207.

ECKMANN, J.-P. & RUELLE, D. 1985 Ergodic theory of chaos and strange attractors. *Rev. Mod. Phys.* **57**, 617.

KEEFE, L., MOIN, P., & KIM, J. 1987 The Dimension of an Attractor in Turbulent Poiseuille Flow. *APS Bull.*. **32**, 2026.

FREDERICKSON, P., KAPLAN, J. L., YORKE, E. D., & YORKE, J. A. The Liapunov Dimension of Strange Attractors J. Diff. Equ. *49.* **185.**

GOLDHIRSCH, I., SULEM, P.-L., & ORSZAG, S. A. 1987 Stability and Lyapunov Stability of Dynamical Systems: A Differential Approach and a Numerical Method. *Physica.* **27D**, 311.

GREENE, J. M., & KIM, J.-S. 1987 The Calculation of Lyapunov Spectra. *Physica.* **24D**, 213.

JIMÉNEZ, J. 1989 Transition to turbulence in two dimensional Poiseuille flow. *J. Fluid Mech.* , (to appear).

MOSER, R. D., MOIN, P., & LEONARD, A. 1983 A Spectral Numerical Method for the Navier-Stokes Equations with Applications to Taylor-

COUETTE FLOW J. Comp. Phys 52. *524.*